MOISTURE INTRUSION IN VISCOELASTIC POROUS MEDIA: INDUCED-STRESS AND DEFORMATION

by

António F. MIGUEL and António HEITOR REIS

Original scientific paper
UDC: 66.081.2:532.546:66.011
BIBLID: 0354-9836, *13* (2009), 1, 47-54
DOI: 10.2298/TSCI0901047M

Porous media exposed to humid air absorb moisture which can lead to extensive internal damage and failure. In this paper, we analyze numerically the influence of the moisture intrusion in a two-layer viscoelastic porous media. The relationship between air humidity and moisture content inside the porous media was examined. It was also found that the local stress increases with the exposure time to humid air but decreases with initial moisture content of the porous medium. Furthermore, the stress components were tensile at the centre of the medium and compressive near the medium surface. The ultimate strength of the medium was only exceeded for the stresses in axial and tangential directions.

Key words: *moisture intrusion, moisture content, stress, failure, porous media*

Introduction

The study of porous media has received considerable attention due to the large number of applications in science and engineering [1, 2]. Moisture intrusion in porous media, besides depending of porous media properties, is related to the conditions of humidity and temperature of the surrounding environment [1-4]. As porous materials absorb and hold moisture, they may be internally affected.

The presence of moisture can cause swelling and high levels of moisture may eventually lead to internal damage and failure [5]. The last occurs when the induced stress exceeds the failure strength of the porous medium. An understanding of stress patterns is very important since porous media may be applied in different technical applications [1, 2]. Despite, moisture-induced stress has received far less attention than fluid transport through porous media, and consequently, the subject still poorly understood [1, 6].

It is difficult to study moisture-induced stress in the laboratory [5, 7]. A model coupling moisture transport and stress balance may permit to calculate in detail the stress distribution in porous media. This paper is an attempt to provide new insight into how stress patterns develop within a porous medium. In this study, moisture intrusion in a two-layer porous medium was modelled based on the approaches of van der Kooi [8] and Miguel [3, 9]. Based on the assumption that the porous medium is viscoelastic (*e. g.*, combines the characteristics of elastic solid and a viscous fluid), an approach was developed for the stress distribution and to predict the occurrence of fissures inside the porous media. The resulting set of equations was solved numerically for a two-layer porous medium. The profile of stresses and strains were computed and the occurrence of fissures analysed.

Theoretical framework

Moisture flux

Consider a porous medium exposed to humid air. In case of thermal equilibrium between the porous medium and the surrounding atmosphere, the steady moisture intrusion Q from the atmosphere to the porous medium surface is given by [2, 8, 10]:

$$Q = \rho\chi(\Theta_{\text{air}} - \Theta_{\text{s}}) \tag{1}$$

with

$$\Theta_{\text{air}} \quad \psi \frac{\rho_{\text{sat}}}{\rho_{\text{dry}}} \tag{2}$$

$$\chi = 10^{-7}\, DL^{-1}\,(5.1 + 1.6\,\text{Re}^{0.5}\,\text{Sc}^{0.33}) \tag{3}$$

$$\chi \quad 2.23\ 10^{\ 5}\ \frac{T}{256}^{\ 1.81} \tag{4}$$

The moisture flux within the porous medium is [1-3, 9, 10]:

$$Q = -\rho D_{\Theta}\ \ \Theta \tag{5}$$

and the rate change of moisture content inside the medium is given by:

$$\rho\dot{\Theta} \quad Q \tag{6}$$

with

$$D_{\Theta} \quad np_{\text{z}}\Theta_{\text{sat}}^{-1}\kappa\ 1 - \frac{T}{T_{\text{z}}}^{\ \text{m}}\ \frac{\Theta}{\Theta_{\text{sat}}}^{\ -\text{n}-1}\ \ \frac{1}{\rho}\eta p_{\text{vs}}\frac{\text{d}\psi}{\text{d}\Theta} \tag{7}$$

where $\dot{\Theta}$ denotes the time derivative of the moisture content.

Stress-strain approach and failure criterion

High levels of moisture inside the porous media may cause swelling and extensive internal damage. For a linear viscoelastic porous medium the relationship between local stress and strain can be written as [5]:

$$\sigma_{t} \quad \beta\varepsilon \quad \beta\xi\dot{\varepsilon}\Delta t \tag{8}$$

where $\dot{\varepsilon}$ represents the time derivative of strain.

Under isothermal conditions, the strain ε is equal to the summation of the viscoelastic component ε_{el} [5, 11] and the hygroscopic component ε_{hy} [9], being this component expressed by:

$$\varepsilon_{\text{hy}} \quad \alpha\Theta - I\Theta_{0} \tag{9}$$

where α represents the linear hygroscopic expansion [12].

According to Christensen [11], the internal displacement of the medium δ is related to the strain ε by:

$$\varepsilon = \omega\delta \tag{10}$$

The study of fissure initiation and propagation requires a failure criterion. This criterion is based on the local strain energy E_{st}. The strain energy is the measure of the energy stored in a medium and is given by [13]:

$$E_{st} = 0.5\,\sigma_t\,\varepsilon_{el} \tag{11}$$

The medium failure is initiated when the strain energy reaches a critical value defined by [13]:

$$E_{st,crt} \quad \frac{c}{K}\sigma_{ult}^2 \tag{12}$$

where σ_{ult} represents the ultimate strength and K is the bulk modulus of the medium.

Problem definition and numerical solution

The porous material depicted in fig. 1 is considered here. The cylindrical-shaped medium comprises inside an ellipsoid-shaped layer, being each one homogeneous and isotropic but made of different materials. This two-layer configuration is common in natural and engineered systems and can be used as a means to create a barrier to migrating fluids [14].

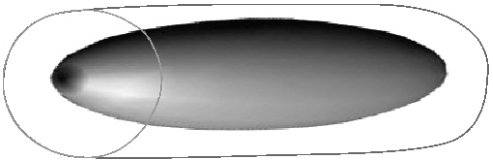

Figure 1. Porous medium composed by cylindrical-shaped and ellipsoid-shaped layers

Computational simulations in the geometry depicted in fig. 1 were performed using a finite-element scheme [15]. A viscoelastic boundary problem is governed by the following relations in a similar manner to the elastic boundary used in general literature [11]:

$$\Theta_s \quad \Theta_{pm} \qquad \text{for } t \quad 0 \tag{13.1}$$

$$D_\Theta \ \Theta \quad \chi(\Theta_s - \Theta_{air}) \quad \text{for } t \quad 0 \tag{13.2}$$

and

$$\sigma + F = 0 \tag{14}$$

where σ is the stress vector and F is the body force vector. The air humidity is prescribed at the surrounding atmosphere while the initial moisture content of the porous medium is also set. A complete and detailed description can be found in [9].

The accuracy of our numerical simulations was validated with respect to refinement and spatial resolution of the grid based on the methodology proposed by Roache [15]. Grids with 12500-135000 tetrahedral cells and 20000--25000 nodes are found to be appropriate for the present study (fig. 2). The solution converged rapidly and monotonically. Convergence was typically achieved around 900 iterations. A complete and detailed description of the solution method can be found in [16, 17].

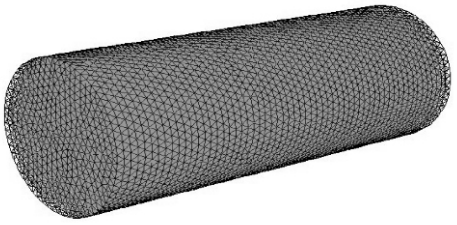

Figure 2. Grid of the domain

Evaluation of the predictive accuracy of the numerical model

As far as is known, experimental investigations on stress distribution in a porous medium composed by cylindrical-shaped and ellipsoid-shaped layers are not available in the litera-

ture. The predictive accuracy of our model is made by comparing our results against experimental obtained by Breuer [18] on a prolate spheroid porous media composed two different layers (length 2.5 cm, diameter 1 cm). The result of this comparison is plotted in tab. 1.

Table 1 indicates that the prediction made with our model is within the accuracy interval of the measurements performed by [18].

Table 1. Radial stress for a prolate spheroid porous media exposed to air with different relative humidity

Air relative humidity [%]	Radial stress [MPa]			
	Initial moisture content 0.035		Initial moisture content 0.071	
	Experiment [18]	Our simulation	Experiment [18]	Our simulation
61	1.1 ± 0.2	0.9	–	0.4
85	2.1 ± 0.5	2.3	1.3 ± 0.3	1.0
98	3.2 ± 0.3	3.4	1.7 ± 0.4	1.9

Foresight study: stress distributions in porous media

Having obtained satisfactory results with the proposed numerical model (section 4.), we were able to use the approach developed in this work to predict the moisture content inside the porous media exposed to humid air, as well as the stress distribution and the fissures occurrence under the influence of the moisture intrusion. The following investigation is intended to provide qualitative features of the moisture intrusion within the porous medium depicted in fig. 1. The cylindrical-shaped medium (radius 1.0 cm, length 5.0 cm) comprises inside an ellipsoid-shaped layer (maximum radius 0.9 cm, length 4.0 cm). In order to perform the simulations the porous medium characteristics and the environmental conditions should be known. Table 2 shows the model parameters for the situations simulated.

Table 2. Model parameters

Porous medium		Surrounding atmosphere	
Temperature [T]	298 K	Temperature [T]	298 K
Constants	$c = 0.17$, $m = 1.2$, $n = 0.14$	Density (ρ)	1.18 kg/m^3
Bulk modulus [K]	$9.6 \cdot 10^{11}$ Pa	Viscosity (μ)	$1.85 \cdot 10^{-5}$ Pa·s
Hygroscopic expansion coefficient (α)	$0.06(\Theta/\Theta_0) + 15$	Reynolds number (Re)	63.8
Relaxation function (ξ)	$8 \exp(-10\,\Theta/\Theta_0)$	Relative humidity (ψ)	0.70 to 0.95
Permeability (κ)	$1 \cdot 10^{-9}$ m^{4}N^{-1}s^{-1} (layer 1) $2 \cdot 10^{-7}$ m^{4}N^{-1}s^{-1} (layer 2)		
Vapour transmission coefficient (a)	$1 \cdot 10^{-7}$ s (layer 1) $2 \cdot 10^{-6}$ s (layer 2)		

First the moisture content within the porous media exposed to different humidity levels was simulated. Figure 3 shows the average moisture content in the porous medium. As expected, the plot indicates that the moisture content increases while the air humidity increases too. Besides, the moisture content has a logarithmic dependence of the air humidity. This result is in agreement with [8, 10].

Once the moisture content inside the porous medium is obtained, stresses and strains are simulated based on eqs. (8) to (14). For convenience the results are presented in terms of a dimensionless parameter Ω that represents the ratio between the local moisture-caused stress σ_t and the failure (tensile or compressive) strength σ_{ult} *vs.* l/L (ratio between the local position and the characteristic dimension considered for the three main directions). The results are plotted in figs. 4 to 9. According to these plots, Ω may be a positive or a negative value. For the point of view of physics, a positive Ω means that material is under tensile tension while a negative value means that the material is under compression. In the absence of fissures Ω varies –1 and 1 ($-1 < \Omega < 1$). Outside of this interval the ultimate (tensile or compressive) strength is exceeded and fissures begin to occur through the medium.

The effect of the relative humidity of the atmosphere that surrounds the porous media, and the time of exposure on the radial, axial, and tangential stresses is shown in figs. 4 to 6.

Figure 4 shows the radial Ω distribution at the central plane of the porous medium, when exposed to air relative humidity of the 0.70 and 0.95, during 12 and 72 hours. The plot indicates that the moisture-caused radial stress is tensile but near the surface of the medium is close to zero. The ultimate strength is not exceeded and consequently fissures cannot occur.

The axial Ω distribution at the central plane of the porous medium is plotted in fig. 5. The plot shows that the stress is compressive near the medium surface and tensile in the remaining parts. The ultimate strength is exceeded at the centre of the medium ($0.38 < l/L < 0.62$), when the porous medium is exposed to a relative humidity of 0.95 for 72 hours. The Ω peak (1.32) occurs right in the middle ($l/L = 0.5$) and indicates that the moisture-caused tensile stress exceed the ultimate strength by 32%.

The tangential Ω distribution on the porous medium when exposed to the air relative humidities of the 0.70 and 0.95 is displayed in

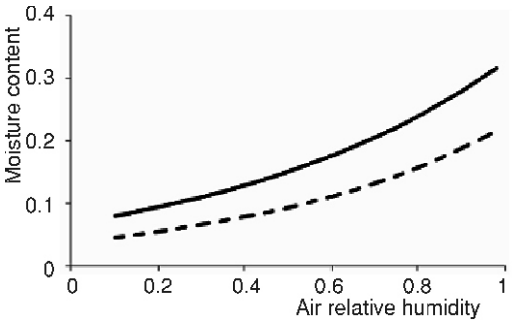

Figure 3. Average moisture content inside the porous media *vs.* air humidity (–– initial moisture content 0.038; — initial moisture content 0.068)

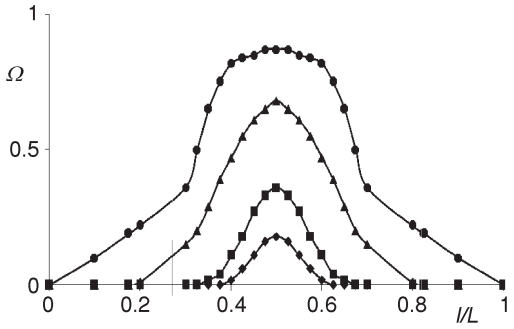

Figure 4. Ratio between the local radial stress and the failure strength (Ω) at central plane of the porous medium; conditions: initial moisture content (Θ_0) 0.07, porous medium exposed to air humidity of 0.70 (◆, ■) and 0.95 (▲, ●) for 12 hours (◆, ▲) and 72 hours (■, ●) of exposure time

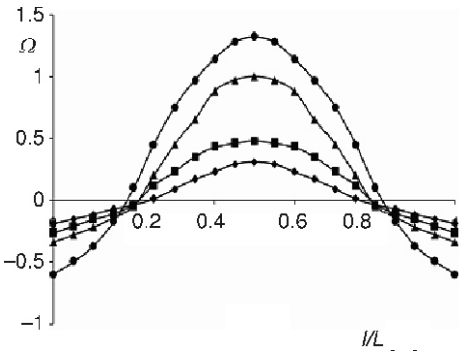

Figure 5. Ratio between the local axial stress and the failure strength (Ω) at central plane of the porous medium; conditions: initial moisture content (Θ_0) 0.07, porous medium exposed to air humidity of 0.70 (◆, ■) and 0.95 (▲, ●) for 12 hours (◆, ▲) and 72 hours (■, ●) of exposure time

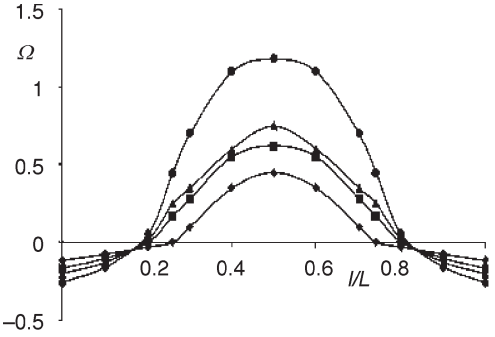

Figure 6. Ratio between the local tangential stress and the failure strength (Ω) at central plane of the porous medium; conditions: initial moisture content (Θ_0) 0.07, porous medium exposed to air humidity of 0.70 (◆, ■) and 0.95 (▲, ●) for 12 hours (◆, ▲) and 72 hours (■, ●) of exposure time

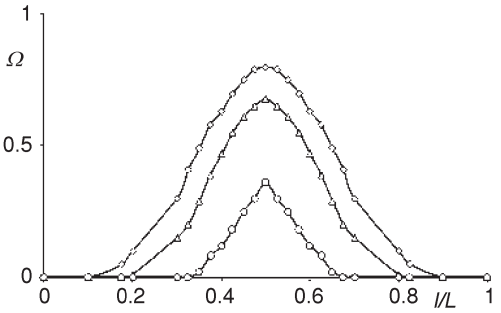

Figure 7. Ratio between the local radial stress and the failure strength (Ω) at the central plane of the porous medium; conditions: exposure time 12 hours, air relative humidity 0.95, initial moisture content 0.04 (◇), 0.07(△), and 0.10 (○)

fig. 6. This plot is similar to fig. 5 and indicates that the moisture-caused stress is tensile all over the direction except near the surface. The failure strength occurs in the tensile zone ($0.36 < l/L < 0.64$). A peak of $\Omega = 1.18$ is reached at $l/L = 0.5$. This means that the maximum local tensile stress exceeds the ultimate tensile strength of the medium by 18%.

According to figs. 5 and 6, the local compressive stress is always smaller than the respective ultimate strength. Therefore, for the cases studied the compressive stress doesn't contribute to the occurrence of fissures. The absolute value of the compressive axial stress distribution (fig. 5) is higher compared to the results obtained for the tangential stress distribution (fig. 6). Consequently, the development of fissures seems more likely to occur in the axial direction than in the tangential direction.

Another parameter that influences the stress distribution is the initial equilibrium moisture content in the porous medium. The resulting axial, tangential, and radial stress components for different values of initial moisture content are plotted in figs. 7 to 9. It is interesting to

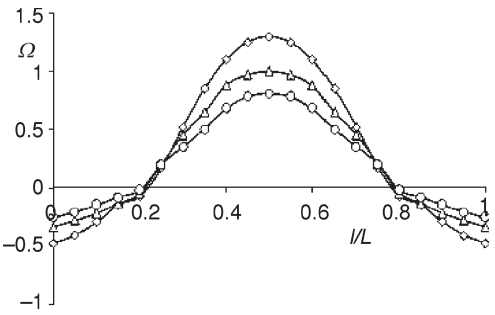

Figure 8. Ratio between the local axial stress and the failure strength (Ω) at the central plane of the porous medium; conditions: exposure time 12 hours, air relative humidity 0.95, initial moisture content 0.04 (◇), 0.07 (△), and 0.10 (○)

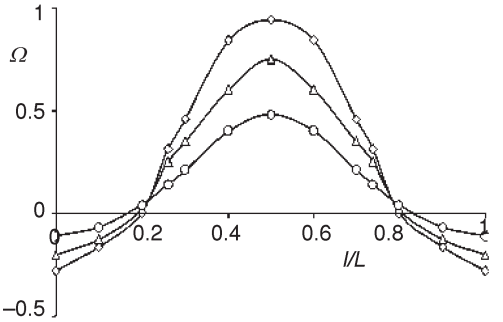

Figure 9. Ratio between the local tangential stress and the failure strength (Ω) at the central plane of the porous medium; conditions: exposure time 12 hours, air relative humidity 0.95, initial moisture content 0.04 (◇), 0.07 (△), and 0.10 (○)

note that Ω decreases when the initial equilibrium moisture content increases. Therefore, a medium having low equilibrium moisture when exposed to high humidity environments may develop fissures more easily (in particular with axial stress) than materials with high equilibrium moisture.

Concluding remarks

The study reported in this paper is devoted to the moisture-caused stress inside a viscoelastic porous medium. A numerical study was developed in a two-layer porous media. The analysis revealed that the moisture content inside the porous medium is a logarithm function of the air humidity. Besides, the study showed that the moisture content inside the porous medium affects the stress distribution inside it. The results also revealed that the local stress increases with exposure time to humid air but decreases with initial equilibrium moisture content of the porous medium. The moisture-induced radial stress is tensile but axial and tangential stress components may be tensile and compressible. The ultimate strength of the medium was only exceeded for the stresses in axial and tangential direction. Consequently, fissures do not occur in radial direction.

Nomenclature

c – constant in eq. (12)
D – air moisture diffusivity, [m^2s^{-1}]
D_Θ – medium moisture diffusivity, [m^2s^{-1}]
E_{st} – strain energy density, [Jm^{-3}]
I – unit tensor
K – bulk modulus, [Pa]
L – characteristic length, [m]
l – local position, [m]
m – constant in eq. (7)
n – constant in eq .(7)
p – pressure, [Pa]
Q – moisture flux density, [$kgm^{-2}s^{-1}$]
Re – Reynolds number, [$\rho uL\mu^{-1}$]
Sc – Schmidt number, [$\mu\rho^{-1}D^{-1}$]
T – temperature, [K]
t – time, [s]
u – air velocity, [ms^{-1}]

Greek symbols

α – linear hygroscopic expansion tensor
β – viscoelastic constitutive stress-strain tensor
δ – internal displacement tensor, [m]
ε – strain tensor
ε_{el} – local elastic strain tensor
ε_{hy} – hygroscopic component of strain tensor, [m]
η – vapour transmission coefficient, [s]
Θ – moisture content
κ – hydraulic permeability, [$m^4N^{-1}s^{-1}$]
μ – dynamic viscosity, [Pa·s]
ξ – relaxation function
ρ – density, [kgm^{-3}]
σ – stress tensor, [Pa]
σ_{ult} – ultimate strength tensor, [Pa]
ψ – air relative humidity, [–]
χ – moisture transfer coefficient from air to surface by diffusion, [ms^{-1}]
Ω – ratio between local moisture-caused stress and failure strength, [–]
ω – strain-displacement gradient matrix, [m^{-1}]

Subscripts

crt – critical value
dry – dry state
el – elastic
pm – porous medium
s – surface
sat – saturated state
t – total
vs – saturation of water vapour
z – at 273 K
0 – initial

References

[1] Nield, D. A., Bejan, A., Convection in Porous Media, 2nd ed., Springer, New York, USA, 1999
[2] Bejan, A., *et al*., Porous and Complex Flow Structure in Modern Technology, Springer, New York, USA, 2004

[3] Miguel, A. F., Contribution to the Characterisation of Porous Media, *Int. J. Heat and Mass Transfer, 43* (2000), 13, pp. 2267-2272
[4] Miguel, A. F., Serrenho, A., On the Experimental Evaluation of Permeability in Porous Media Using a Gas Flow Method, *Journal of Physics D, 40* (2007), 21, pp. 6824-6828
[5] Hearn, E. J., Mechanics of Materials 2, Butterworth Heinemann, Oxford, UK, 1997
[6] Augier, F., *et al*., On the Risk of Cracking in Clay Drying, *Chemical Engineering Journal, 86* (2002), 1-2, pp. 133-138
[7] Muralidharan, V., *et al*., A Flow Through Porous Media Model for Pore Pressure During Heating of Polymer–Matrix Composites, *Composites Science and Technology, 66* (2006), 10, pp. 1409-1417
[8] van der Kooi, J., Moisture Transport in Cellular Concrete Roofs, Ph. D. thesis, Eindhoven Technische Hogeschool, Eindhoven, The Netherlands, 1971
[9] Miguel, A. F., Transport Phenomena through Porous Screens and Openings, Ph. D. thesis, Wageningen University and IMAG, Wageningen, The Netherlands, 1998
[10] Wang, B., Yu, W., A Method for Evaluation of Heat and Mass Transport Properties of Moist Porous Media, *Int. J. Heat and Mass Transfer, 31* (1998), 5, pp. 1005-1009
[11] Christensen, R. M., Theory of Viscoelasticity: An introduction, Academic Press, New York, USA, 1982
[12] Bear, J.: Dynamics of Fluids in Porous Media, Dover Publications Inc., New York, USA, 1988
[13] Oore, M., Assessment of Influence Function for Elliptical Cracks Subjected to Uniform Tension, *ASTM Fracture Mechanics,* No. 1074, 1990, pp. 490-508
[14] Loggia, D., *et al*., Phase Diagram of Stable Miscible Displacements in Layered Porous Media, *Europhysics Letters, 36* (1996), 2, pp. 105-110
[15] Roache, P. J.: Verification and Validation in Computational Science and Engineering, Hermosa Publishers, Albuquerque, N. Mex., USA, 1998
[16] Silva, A., Coelho, P. J., Numerical Investigation of Natural Convection in a Rectangular Cavity with an Internal Partition, *Proceedings*, 7th International Conference on Computational Methods and Experimental Measurements, Capri, Italy, Computational Mechanics Publications (Ed. G. Carlomagno), 1995, pp. 18-25
[17] Miguel, A. F., Silva, A., Particle Deposition onto a Flat Plate with Various Slopes, *Journal of Aerosol Science, 34* (2003), supplement 1, pp. 667-668
[18] Breuer, J. J., Moisture and Stress Analysis of Low Porosity Media, Report No. P097-XIX, IMAG, Wageningen, The Netherlands, 1997, p. 58

Authors´ affiliations:

A. F. Miguel (**corresponding author**)
Department of Physics and Évora Geophysics Center,
University of Évora
59, Rua Romao Ramalho, 7000-671 Évora, Portugal
E-mail: afm@uevora.pt

A. H. Reis
Department of Physics and Évora Geophysics Center, University of Évora
Évora, Portugal

Paper submitted: November 27, 2007
Paper revised: July 15, 2008
Paper accepted: December 8, 2008